PNAS RESEARCH ARTICLE | CELL BIOLOGY

Mechanosensitive stem cell fate choice is instructed by dynamic fluctuations in activation of Rho GTPases

Rocío G. Sampayo[a,b], Mason Sakamoto[a,b], Madeline Wang[a,b], Sanjay Kumar[a,b,1], and David V. Schaffer[a,b,1]

Edited by David Weitz, Harvard University, Cambridge, MA; received December 2, 2022; accepted April 24, 2023

During the intricate process by which cells give rise to tissues, embryonic and adult stem cells are exposed to diverse mechanical signals from the extracellular matrix (ECM) that influence their fate. Cells can sense these cues in part through dynamic generation of protrusions, modulated and controlled by cyclic activation of Rho GTPases. However, it remains unclear how extracellular mechanical signals regulate Rho GTPase activation dynamics and how such rapid, transient activation dynamics are integrated to yield long-term, irreversible cell fate decisions. Here, we report that ECM stiffness cues alter not only the magnitude but also the temporal frequency of RhoA and Cdc42 activation in adult neural stem cells (NSCs). Using optogenetics to control the frequency of RhoA and Cdc42 activation, we further demonstrate that these dynamics are functionally significant, where high- vs. low-frequency activation of RhoA and Cdc42 drives astrocytic vs. neuronal differentiation, respectively. In addition, high-frequency Rho GTPase activation induces sustained phosphorylation of the TGFβ pathway effector SMAD1, which in turn drives the astrocytic differentiation. By contrast, under low-frequency Rho GTPase stimulation, cells fail to accumulate SMAD1 phosphorylation and instead undergo neurogenesis. Our findings reveal the temporal patterning of Rho GTPase signaling and the resulting accumulation of an SMAD1 signal as a critical mechanism through which ECM stiffness cues regulate NSC fate.

mechanobiology | Rho GTPases | stem cells | optogenetics | mechanosensing

Significance

Mechanical properties of the microenvironment strongly influence stem cell fate. In general, cells sense and decode such mechanical stimuli through dynamic membrane protrusions controlled by Rho GTPases. However, whether Rho GTPases are activated statically or dynamically in stem cells, as well as how such fast, reversible events may be integrated into irreversible fate decisions, remain unknown. We found that substrate stiffness modulates the frequency of Rho GTPase activation and generation of protrusions in adult neural stem cells. Moreover, using optogenetic Rho GTPase activation, we found that this frequency determines the persistence of SMAD1 activation, which in turn modulates lineage commitment and promotes astrogenesis. Our results thus elucidate a mechanism for temporal integration of dynamic mechanosensing pathways into irreversible fate determination.

From early embryogenesis into adulthood (1, 2), the concerted action of stem cell division and differentiation builds and maintains tissue homeostasis. Differentiation of stem cells into specific lineages is orchestrated by complex biochemical and biophysical signals that vary temporally and spatially (3–5). For example, mechanical signals in stem cell niches can fluctuate due to transient changes in cell density, induced by cell proliferation and migration, as well as the dynamic deposition of specific extracellularmatrix (ECM) molecules by these cells (6). In addition, it has been proposed that cells sense and decode ECM mechanical cues into intracellular signals by generating membrane protrusions in the order of seconds to minutes, exerting force and deforming underlying physical structures, processes by which cells can repeatedly and locally probe the viscoelastic properties of their environment (4, 7). Moreover, substrate stiffness has been shown to determine the morphology and dynamics of these exploratory membrane protrusions in several cell types (4, 7, 8). However, whether static substrate stiffnesses affect these dynamic cytoskeletal processes and accompanying activation of signals such as Rho GTPases in stem cells, and whether such fast, reversible mechanisms can be integrated into long-term, irreversible effects on cell fate commitment, are still largely unknown.

The waves of exploratory protrusions are thought to arise due to nonspecific adhesion mechanisms (9, 10), triggering downstream contraction/relaxation events of the acto-myosin cytoskeleton that are controlled by Rho family of GTPases (11). The reversible nature of Rho GTPases, which switch between guanosine triphosphate (GTP)-bound active and guanosine diphosphate (GDP)-bound inactive states (12), enables cells to sustain cycles of extension and retraction of protrusions, critical for mechanosensing as well as directional migration. These GTPases play critical roles in controlling rapid cytoskeletal network effects as well as long-term signal transduction events that determine gene expression and ultimately determine cell fate (4, 13).

We previously showed that ECM stiffness instructs cell fate in adult hippocampal neural stem cells (NSC) via a mechanism involving the Rho GTPases RhoA and Cdc42 (3, 14, 15). These NSCs reside in the subgranular zone (SGZ) of the hippocampus and give rise to neurons and glia that play critical roles in learning, memory, and pattern recognition (16, 17). SGZ NSCs live at the interface between two hippocampal layers with sharply different stiffnesses, which likely exposes them to diverse mechanical inputs (18, 19). We showed in vitro that NSCs exhibit mechanical memory, wherein they are sensitive to the elastic properties of the substrate between the first 12 to 36 h of differentiation in culture,

Preprint Server: bioRxiv.

Author contributions: R.G.S., S.K., and D.V.S. designed research; R.G.S., M.S., and M.W. performed research; R.G.S., S.K., and D.V.S. contributed new reagents/analytic tools; R.G.S. and M.S. analyzed data; S.K. and D.V.S. revised and edited the manuscript; and R.G.S. wrote the paper.

The authors declare no competing interest.

This article is a PNAS Direct Submission.

[1]To whom correspondence may be addressed. Email: skumar@berkeley.edu or schaffer@berkeley.edu.

This article contains supporting information online at https://www.pnas.org/lookup/suppl/doi:10.1073/pnas.2219854120/-/DCSupplemental.

Published May 22, 2023.

after which they are irreversibly committed to a specific fate that arises 4 to 6 d later (14, 15). Other stem cell types such as mesenchymal stem cells (MSCs) also exhibit mechanical memory, and Rho GTPase activity has also been shown to be critical for lineage commitment (20, 21). However, it remains unknown whether static ECM stiffnesses produce static or dynamic activation of Rho GTPases, and whether dynamic activation could be integrated into long-term, persistent signal transduction events necessary to irreversibly determine cell fate beyond the temporal window of mechanosensitivity.

Using NSCs as a model for adult multipotent stem cells, we show that ECM stiffness determines not only the magnitude but, strikingly, also the frequency of Rho GTPase oscillatory activation, with stiffer substrates promoting higher activation frequencies. We then employed optogenetically controlled RhoA and Cdc42 variants we previously developed (22) to investigate how this mechanosensitive oscillatory activation of Rho GTPases influences NSC fate decisions. Combining this technology with single-cell differentiation profiling, we reveal that NSC fate commitment is determined by the frequency of oscillatory activation of RhoA and Cdc42 during a critical temporal window. High-frequency activation resulted in persistent actin cytoskeleton subcellular reorganization and downstream phosphorylation and nuclear translocation of SMAD1/5, a transcription factor that promotes astrocytic differentiation. By contrast, low-frequency activation yielded only intermittent activation of SMAD1/5 that was insufficient to promote astrocytic fates and instead favored neuronal differentiation. ECM stiffness thus determines the frequency of Rho GTPase activation, and these dynamic signaling inputs are temporally integrated, through actin cytoskeleton and SMAD1/5 dynamics, into irreversible stem cell fate decisions.

Results

ECM Stiffness Controls the Frequency of Oscillatory RhoA Activation in Adult NSCs. To investigate how ECM stiffness regulates RhoA activation in adult multipotent stem cells, we engineered adult hippocampal NSCs to express a previously described fluorescence resonance energy transfer (FRET)–based RhoA biosensor (23) that enables quantification of RhoA activity via live-cell imaging (Fig. 1*A*). Polyacrylamide (PA) hydrogels that are tunable over a broad range of stiffnesses encompassing the stiffness range of brain tissue and covalently conjugated the surfaces with laminin were used (24). We then measured RhoA activation dynamics during the critical temporal window of mechanosensitivity we previously identified for these cells (12 to 36-h after induction of differentiation on PA gels) (15) in the presence of biochemical cues that over 7 d induce mixed differentiation into primarily neurons and astrocytes (14) (Fig. 1*B*). Ratiometric FRET analysis revealed that cells on either soft (528 Pa) or stiff (73 kPa) PA hydrogels exhibited localized subcellular regions or "domains" of RhoA activation that were distributed throughout the cytoplasm and plasma membrane (*SI Appendix*, Fig. S1 *A* and *B*). Regions with high (average FRET index amplitude ≥ 0.4) and low RhoA activation (average FRET index amplitude ≤ 0.2) were identified on both substrates. Interestingly, stiff substrates exhibited more regions with high RhoA activity, whereas soft substrates showed more regions with low activity, consistent with our previous ELISA-based GTPase-activation assay measurements indicating ~1.8-fold higher activity of RhoA on stiff substrates (14) (Fig. 1*C* and *SI Appendix*, Fig. S1*C*). However, temporal analysis of RhoA activation within different regions (~400 nm in diameter [Fig. 1*D*], see *SI Appendix*, *Additional Materials and Methods* for details) strikingly revealed an oscillatory pattern in RhoA activation with significantly different frequencies on soft vs. stiff substrates (Fig. 1 *C*, *E*, and *F*). That is, NSCs seeded on soft substrates had peaks of RhoA activation every ~45 to 60-min, whereas RhoA activation peaked every 5 to 10 min on stiff substrates (Fig. 1 *D*–*F*). RhoA activation thus spontaneously oscillated in NSCs at a frequency modulated by the elastic properties of the substrate (Fig. 1*G*). Given our prior observations that NSC fate varies continuously with substrate stiffness, where substrates of elastic modulus >1.5 kPa render significant inhibition of neurogenesis (14), we investigated whether RhoA activation dynamics followed an analogous trend. Interestingly, cells seeded on a substrate of 1.5 kPa exhibited an intermediate response between that observed on 528 Pa and 73 kPa, with an average period of activation of RhoA of ~18-min (*SI Appendix*, Fig. S1*D*). These findings suggest that not only cell fate commitment but also RhoA activation dynamics are sensitive to variations in elastic modulus, particularly on softer (500 to 1,500 Pa) matrices.

We have previously shown that not only RhoA but also Cdc42 GTPase is involved in mechanosensitive NSC lineage commitment (14). Therefore, we evaluated the presence of temporal fluctuations in Cdc42 activation on NSCs seeded on substrates of varying stiffness. Remarkably, Cdc42 activation followed comparable mechanosensitive fluctuations, with an average period of 38.3 min on soft (528 Pa) substrates and 8.4 min on stiff substrates (73 kPa) (*SI Appendix*, Fig. S1 *E* and *F*).

We further assessed whether protrusion frequency, which we would expect to be closely connected to RhoA activation, may be sensitive to substrate elasticity. We found that the number/cell of either newly formed or retracted cellular protrusions in the time scale of RhoA/Cdc42 activation (15-min windows) increases with substrate stiffness, while the number/cell of membrane protrusions of unchanged length remains constant (*SI Appendix*, Fig S2 *A*–*C*). Moreover, we found that on stiff substrates, cells exhibit a pattern of oscillatory neurite extension with a period of 6-min, comparable to the 5 to 10-min gap between peaks of RhoA activation when cells are seeded on these substrates (*SI Appendix*, Fig S2 *A* and *D*). On soft substrates, we were not able to detect neurite reextension after retraction (or neurite retraction after extension) within the temporal window analyzed, suggesting that if there is an oscillatory pattern of neurite extension on soft substrates, the period would be longer than the analyzed timeframe. These data suggest that NSCs exhibit oscillatory patterns of neurite extension and retraction, and that the frequency of these oscillations is modulated by substrate stiffness. These fast, spontaneous bursts of neurite extension/retraction found on stiff substrates may contribute to high-frequency oscillatory RhoA activation in NSCs.

Optogenetic RhoA and Cdc42 Enable High Spatiotemporal Resolution Control of GTPase Activation in NSCs. Having found that ECM stiffness modulates not only the average magnitude but also the frequency of RhoA activation, we wondered whether Rho GTPase oscillation frequency could impact NSC fate commitment. Strategies to manipulate Rho GTPase activation such as biochemical activators of Rho GTPase pathways (lysophosphatidic acid (LPA) or calpeptin) lack temporal resolution due to cellular diffusion constraints. Moreover, genetic perturbation of Rho GTPases typically involves expression of constitutively active or dominant negative mutants, which also lack rapid temporal tunability. To overcome these limitations, we previously placed RhoA and Cdc42 under optogenetic control (25), enabling Rho GTPase activation with high spatiotemporal resolution. In this system, full-length RhoA or Cdc42 is fused to a truncated *Arabidopsis Thaliana* Cryptochrome 2 (Cry2), hereafter named "optoRhoA" and "optoCdc42," such that

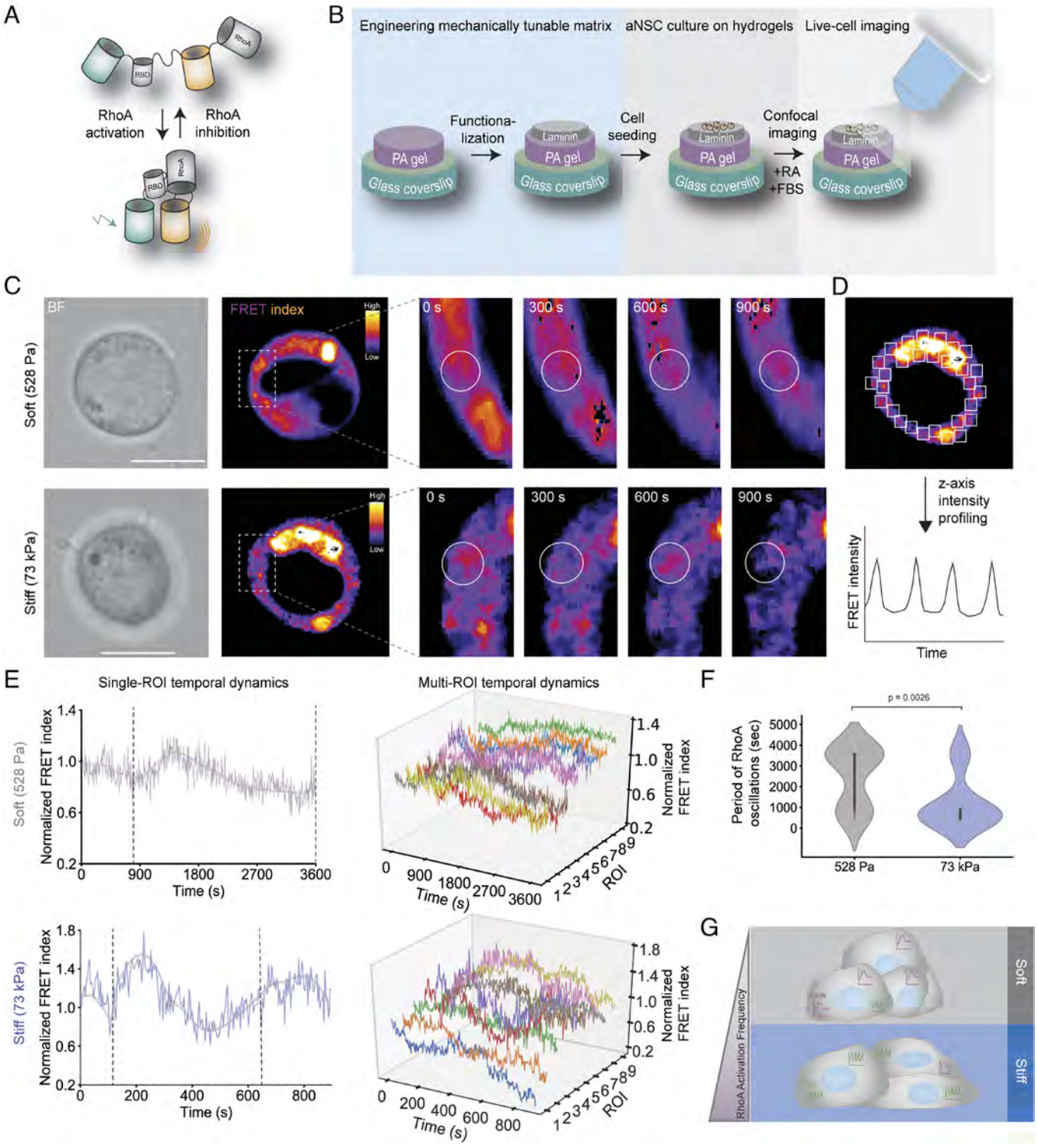

Fig. 1. Frequency of RhoA activation is modulated by substrate elasticity in NSCs. (*A*) Representation of the FRET biosensor. (*B*) Hydrogel model of tunable stiffness (*C*) Temporal dynamics of RhoA activation measured by a single-chain FRET biosensor in NSCs. High FRET-index represents high degree of activation of RhoA. (Scale bar, 10 μm.) (*D*) FRET-index temporal profile was tracked in 20 ROIs/cell (400 nm^2 squares); 10 cells/condition were analyzed. (*E*) Temporal profile of FRET-index in cells seeded on soft or stiff substrates. *Left* column: representative temporal profile for single-ROI dynamics. *Right* column: representative FRET temporal dynamics across 10 ROIs in all cells analyzed. FRET-index at each timepoint was normalized to $t = 0$. Temporal FRET-index profiles were used to calculate oscillation frequencies as described in *Materials and Methods*. (*F*) Distribution of RhoA activation frequency between soft and stiff. Student's *t* test was used to evaluate significance. (*G*) Stiffness-dependent RhoA oscillatory activation in NSCs. Domains with high-frequency activation of Rho GTPases are more abundant when NSCs are seeded on stiff substrates.

blue-light illumination induces clustering of Cry2 and the activation of the accompanying Rho GTPase (25) (Fig. 2*A*).

To precisely control the amplitude and frequency of illumination for optostimulation, we used our recently reported, programmable photostimulation devices for light activation at variable amplitudes ("LAVA" boards) (26, 27) (Fig. 2*B*). These devices allow for controlled illumination of multiwell plates in routine cell culture, at user-defined frequencies (10-ms resolution) and amplitudes (0.005 μWmm^2 resolution) that are specified independently for each well. Cells were seeded on soft (528 Pa) PA

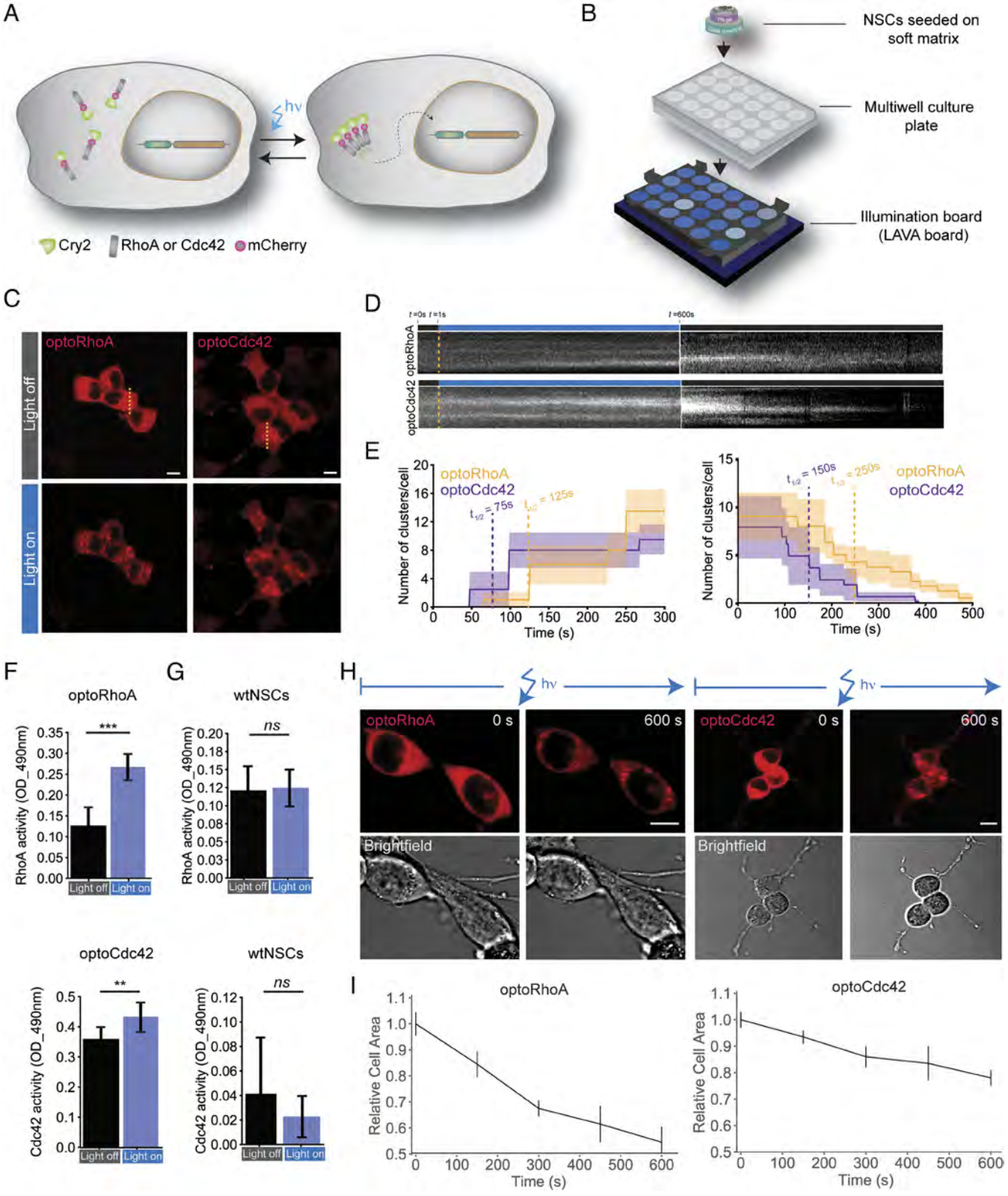

Fig. 2. Optogenetic RhoA and Cdc42 for optical control of GTPase dynamic activation in NSCs. (*A*) Optogenetic RhoA/Cdc42 pathway activation ("optoRhoA" or "optoCdc42") in NSCs. (*B*) LAVA board for optostimulation. (*C*) Live-cell imaging of mCherry-optoRhoA or mCherry-optoCdc42 at $t = 0$ (*Top*) or after 15 min of blue-light stimulation (*Bottom*). Scale bar, 10 μm (*D*) Kymographs of mCherry-optoRhoA or mCherry-optoCdc42 corresponding to the dashed line. (*E*) Representative plot of single-cell cluster formation and dissociation over time. (*F*) Rho and Cdc42 activity measured by ELISA-based GTPase activation assays (G-LISA) after 10 min of blue-light stimulation at 0.5 mW/mm^2 of optoRhoA or optoCdc42 NSCs on soft substrates. Data are mean ± SD (n = 6 biological replicates) (*G*) Rho and Cdc42 activation measured by G-LISA in wtNSCs after 10 min of blue-light stimulation at 0.5 μW/mm^2. Data are mean ± SD (n = 6 biological replicates). (*H*) Time-lapse images of optoRhoA and optoCdc42 NSCs upon 10-min optostimulation. Changes in cell area measured with the software Fiji. Areas were plotted relative to $t = 0$. (Scale bar, 10 μm.) (*I*) Quantification of *H*. Data are mean ± SD (n = 50 cells per condition). ***$P < 0.005$, **$P < 0.01$, *$P < 0.05$. ns = not significant by Student's *t* test.

hydrogels (Fig. 2*B*), which provide the lowest average activation background for RhoA and Cdc42 (Fig. 1*C*) (14). Blue-light stimulation induced clustering and plasma, perinuclear, and membrane localization of these proteins, coinciding with previous reports of active Rho GTPase subcellular distribution (12, 25). Clustering association ($t_{1/2}$ Cdc42 = 75s, $t_{1/2}$ RhoA = 125s) and dissociation kinetics ($t_{1/2}$ Cdc42 = 150s, $t_{1/2}$ RhoA = 250s) were consistent with our prior work in fibroblasts (25) (Fig. 2 *C*–*E*) and in a temporal range useful for simulating endogenous Rho GTPase fluctuations seen in NSCs (Fig. 1).

ELISA-based GTPase activation assays showed a nearly twofold activation of RhoA and ~1.3-fold activation of Cdc42 upon static illumination of optoRhoA and optoCdc42, respectively (Fig. 2*F*), in contrast to wild-type NSCs (wtNSCs) in which no elevation was observed upon illumination (Fig. 2*G*). The degree of activation of RhoA and Cdc42 observed with our optogenetic model resembles the described degree of activation of these proteins (~1.8-fold) when exposed to stiff substrates compared to their baseline activation on soft substrates (14). To examine the functional consequences of optogenetic RhoA or Cdc42 activation, we first evaluated morphological effects. A short (10-min) pulse of light was sufficient to trigger fast cellular contraction in optoRhoA cells (Fig. 2 *H* and *I*), with milder cellular contraction with optoCdc42 (Fig. 2 *H* and *I*). wtNSCs did not show morphological effects when exposed to blue light (*SI Appendix*, Fig. S2*E*). These results validate the use of this light-induced oligomerization system for rapid activation of RhoA and Cdc42, which increased cellular contractility as described for these proteins in NSCs (14) and other cell types (28, 29).

Oscillatory Rho GTPase Activation Instructs Adult NSC Fate. We next analyzed the effects of optogenetic activation of RhoA and Cdc42 on stem cell lineage commitment. After allowing cells to adhere for 18-h in proliferation media, cultures were switched to differentiation media and illuminated with blue light at 0.5 μW/mm^2 for 18-h, within our previously identified critical mechanosensitive window (15). Cell fate was analyzed after an additional 6 d, using βIII-tubulin (a.k.a. Tuj1) as a neuronal marker and glial fibrillary acidic protein (GFAP) as an astrocytic marker (Fig. 3*A*). This 18-h continuous RhoA or Cdc42 activation was sufficient to inhibit neurogenesis and promote astrogenesis in both optoRhoA and optoCdc42 cells (Fig. 3 *B* and *C*), consistent with our prior reports that stiff matrices or constitutively active Rho GTPases suppress neuronal differentiation (3, 14). Illumination did not affect wtNSC fate (*SI Appendix*, Fig. S2 *F* and *G*).

To simulate the Rho GTPase oscillations we observed on stiff and soft gels (Fig. 1), we examined the effect of pulsatile RhoA and Cdc42 activation during the critical temporal window (Fig. 3*D*). We performed a frequency sweep analysis ranging from 15-min to 90-min square pulses of light (duty cycle 50%) and doubled the illumination intensity (1 μW/mm^2) such that light dose was constant for all treatments including the continuous 18-h light condition (Fig. 3*E*). While slightly slower than the frequency observed on stiff substrates (Fig. 1*F*), we chose 15-min square pulses as the fastest frequency tested considering the clustering/dissociation kinetics of these proteins shown in Fig. 2 (~4-min for nearly complete protein clustering and ~8-min for nearly complete dissociation). Strikingly, we found that stem cell fate is sensitive to the frequency of activation of RhoA and Cdc42, with high frequencies inhibiting neurogenesis and promoting astrogenesis to the same extent as continuous illumination (Fig. 3 *F* and *G*). In contrast, 45-min or slower square pulses had the same outcome as cells that did not receive light stimulation (Fig. 3 *F* and *G*). Notably, the proportions of neurons and astrocytes varied continuously with stimulation frequency (Fig. 3*G*). Overall, these data suggest that Rho GTPases encode their capacity to regulate NSC fate in the frequency of their activation, which in turn is determined by the elasticity of the underlying ECM. For further experiments, we chose 45-min square pulses as a stimulation condition that resembles the timeframe of dynamic Rho GTPase activation seen on soft (528 Pa) substrates (~45 to 60 min period) and 15-min square pulses as a stimulation condition comparable to that observed on stiff (73 kPa) substrates (~5 to 10-min period).

We next investigated whether the dynamic activation of these GTPases was instructing cell fate as opposed to selecting a subpopulation of already-committed progenitors though differentially modulating their proliferation or apoptosis. As we previously reported (3, 14), the majority of individual NSCs have the capacity to generate neurons, astrocytes, and, to a lesser extent, oligodendrocytes. To examine clonal cell behavior at different stimulation frequencies, a microisland array technology we previously developed (30) was used to place a single cell in each island and thereby track single-cell fate decisions upon blue-light stimulation (Fig. 4 *A* and *B*). Specifically, using DNA-programmed adhesion, cells were patterned at a density of 1cell/microisland, illuminated with high (15-min square pulses) or low (45-min square pulses) light frequencies over an 18-h period, and analyzed through differential marker expression after 7 d. wtNSCs gave rise to a distribution of lineage commitments—~50% neurons and ~30% astrocytes—that did not vary significantly with the frequency of illumination (Fig. 4 *D* and *E*). In contrast, upon illumination of optoRhoA and optoCdc42 cells for 18 h at different frequencies, the proportion of neurons vs. astrocytes was strongly dependent on stimulation frequency, with microislands harboring 50 to 70% neurons upon low-frequency stimulation and, strikingly, 95 to 100% astrocytes upon high-frequency stimulation (Fig. 4 *C*–*E*). Of note, among microislands that were 100% neuronal or 100% astrocytic, the former had more cells than the astrocytic islands, consistent with previous reports that neuronal but not astrocytic-committed progenitor cells undergo additional proliferation after fate commitment (31). This explains the even more dramatic inhibition of neurogenesis and promotion of astrogenesis seen in this clonal assay compared to the bulk-population assays (Fig. 3 *B* and *F*) upon RhoA or Cdc42 activation. This clonal analysis thus reveals that high-frequency Rho GTPase activation shifts most stem cells toward astrocytic fates, with a small proportion of neuronal committed cells.

Frequency-Dependent Activation of Rho GTPases Controls Downstream Actin Dynamics and Mimics the Effects of Substrate Stiffness on Cytoskeletal Organization. We have previously shown that the downstream contractile and cytoskeletal machinery activated by RhoA and Cdc42 is necessary to mediate stiff substrate inhibition of neurogenesis (14). To determine whether and how frequency-dependent lineage commitment depends on actin assembly, we seeded optoRhoA and optoCdc42 NSCs on compliant (528 Pa) substrates and illuminated at low (45-min square pulses) or high frequencies (15-min square pulses) in the presence of cytochalasin D (CytoD) to inhibit actin polymerization during the critical 18-h window (starting 18-h postseeding and finishing 36-h postseeding) (*SI Appendix*, Fig. S3*A*). This inhibition during the lineage commitment window rescued neurogenesis and suppressed astrogenesis in both optoRhoA and optoCdc42 cells stimulated at high frequencies (*SI Appendix*, Fig. S3 *B* and *C*). We next examined the immediate, short-term effects of RhoA or Cdc42 pulsatile activation on actin dynamics. optoRhoA and optoCdc42 NSCs were engineered to express LifeAct-mVenus to allow for live-cell tracking of actin

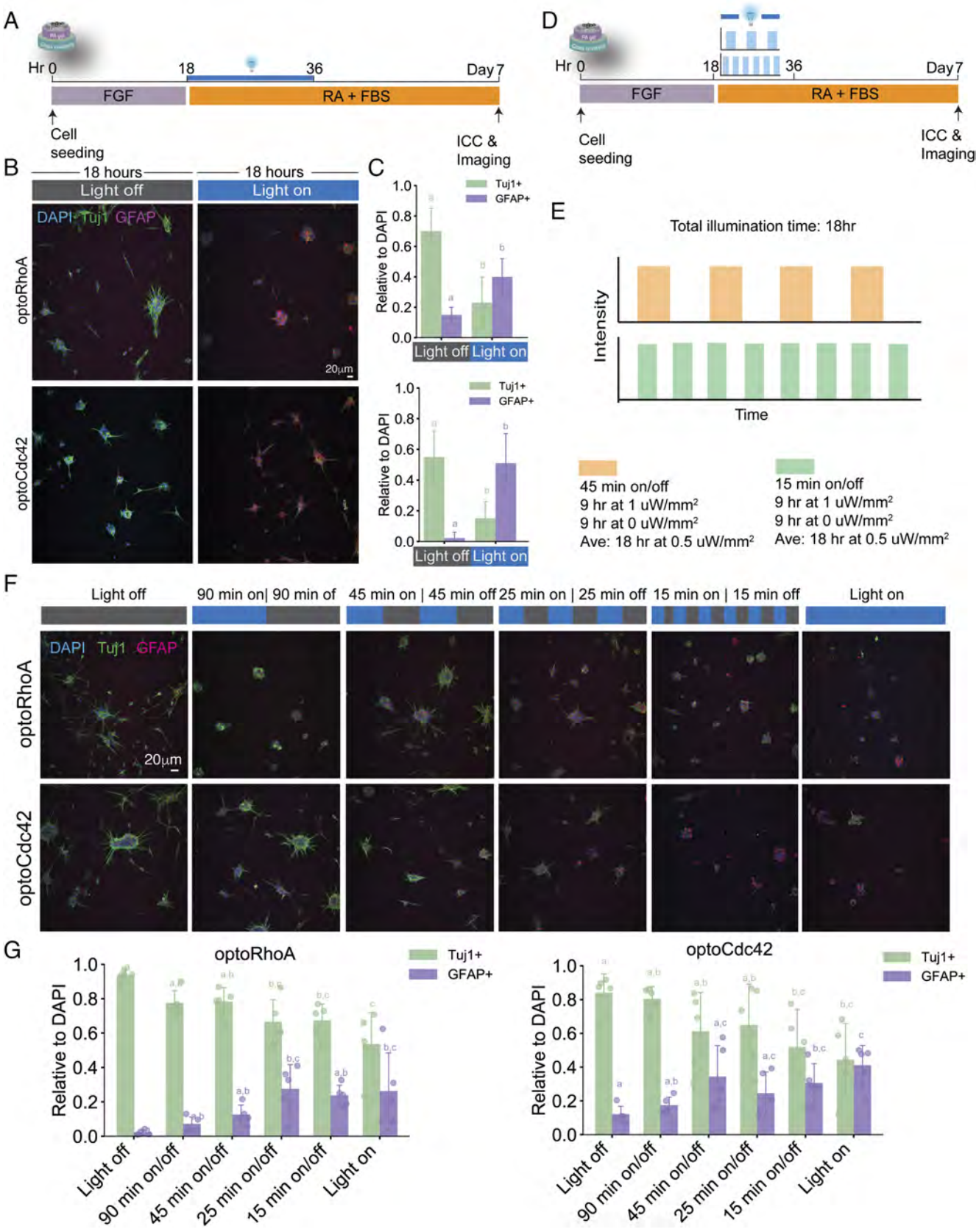

Fig. 3. NSC fate is determined by the frequency of activation of Rho GTPases during a critical temporal window. (*A*) Media conditions and optostimulation pattern used in *B*. (*B*) Immunostaining for Tuj1(neurons), GFAP(astrocytes), or DAPI(nuclei) of optoRhoA or optoCdc42 NSCs after 7 d of differentiation, optostimulated for the first 18 h at a dose of 0.5 μW/mm^2. (*C*) Quantification of *B*. Tuj1+/DAPI and GFAP+/DAPI ratios were calculated. Data are mean ± SD (n = 6 biological replicates). (*D*) Media conditions and optostimulation pattern used in *E*. (*E*) Optostimulation using LAVA boards allows for independent tuning of frequency and amplitude of the applied stimuli. (*F*) Immunostaining of optoRhoA or optoCdc42 NSCs after 7 d of differentiation and optostimulated for the first 18 h at different frequencies, keeping average dose of 0.5 μW/mm^2. (*G*) Quantification of *F*. Tuj1+/DAPI and GFAP+/DAPI ratios were calculated. Data are mean ± SD (n = 6 biological replicates). One-way ANOVA with Tukey's multiple comparison test used to evaluate significance.

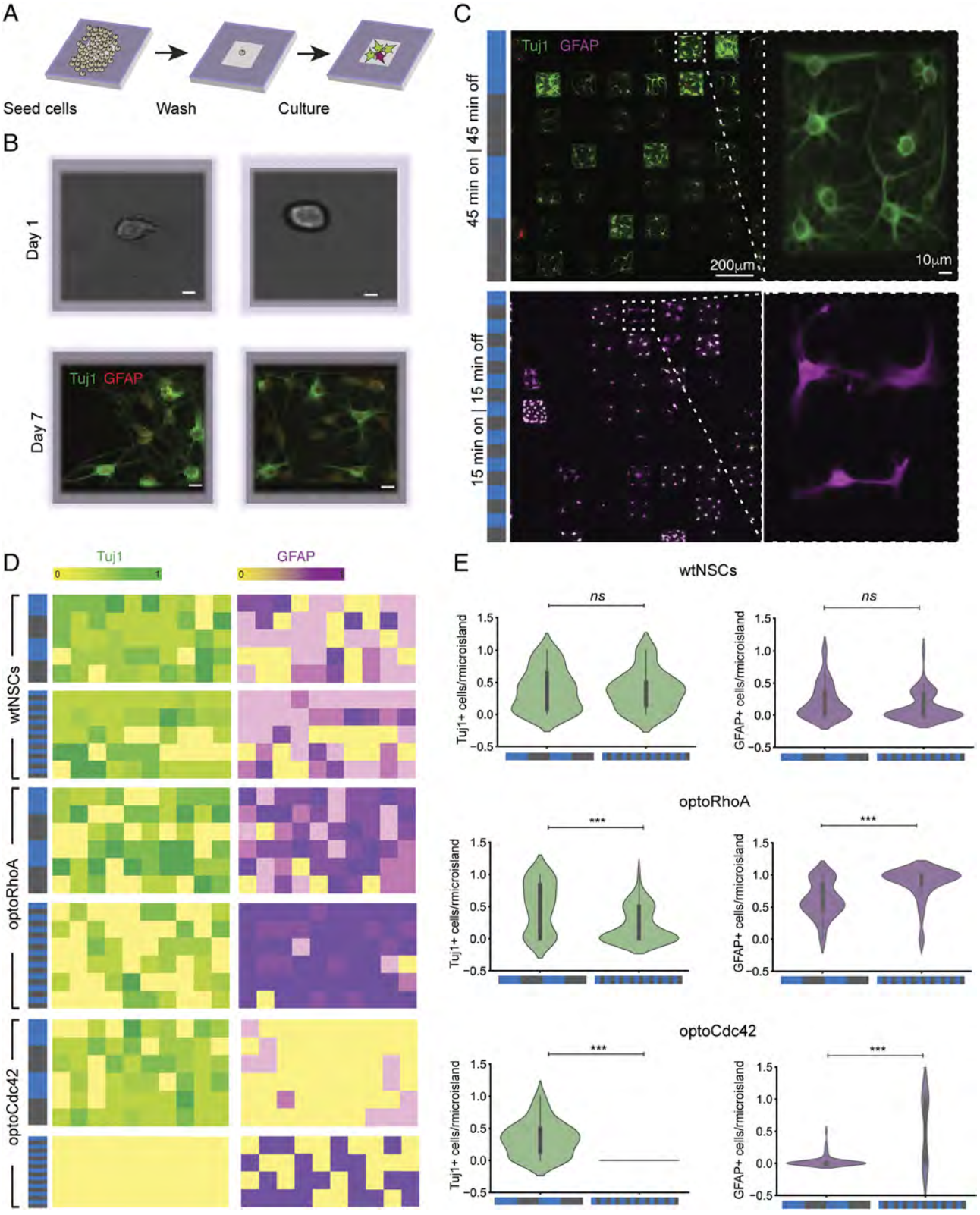

Fig. 4. High-frequency Rho GTPase activation promotes astrogenesis through an instructive mechanism. (*A*) Schematic representation of NSC seeding process onto single-cell microisland arrays. (*B*) Live-cell images (day 1) from 2 microislands and corresponding immunofluorescence staining (day 7). (Scale bar, 10 μm.) (*C*) Immunofluorescence staining of optoRhoA cells seeded in microislands and differentiated for 7 d. (*D*) Heatmaps indicating the proportion (in a 0 to 1 scale) of Tuj1+ or GFAP+ cells relative to DAPI in each microisland. (*E*) Distribution of Tuj1+/DAPI and GFAP+/DAPI ratios per microisland. ***$P < 0.005$, **$P < 0.01$, *$P < 0.05$. ns = not significant by Student's *t* test.

dynamics (*SI Appendix*, Fig. S3*D*). A 15-min pulse of blue light on optoRhoA or optoCdc42 NSCs triggered fast actin disassembly from filopodia-like protrusions and a reorganization around the cortical region and perinuclear compartment (*SI Appendix*, Fig. S3 *E* and *F*), followed by retraction of these protrusions, consistent with increased cellular contractility (*SI Appendix*, Fig. S3*G*). Moreover, clusters of RhoA and Cdc42 formed during these short light pulses and colocalized with actin bundles both in the

plasma membrane and in the perinuclear region (*SI Appendix*, Fig. S3*H*). Altogether, these data indicate that activation of Rho GTPases triggered fast reorganization of actin bundles within different subcellular regions, both the cortical area and perinuclear compartment, and that actin polymerization is necessary to mediate the effects of oscillatory activation of RhoA and Cdc42 on cell fate (*SI Appendix*, Fig. S3*I*).

To further explore the effects of Rho GTPase pulsatile activation on the temporal dynamics of actin cytoskeleton of NSCs, we analyzed actin velocity via live-cell imaging following the design described above (*SI Appendix*, Fig. S3*D*). We found that optogenetic stimulation of RhoA or Cdc42 for the first 15 min decreased actin velocity compared to nonilluminated cells, suggesting that activation of RhoA or Cdc42 immobilizes a pool of cytoplasmic actin (*SI Appendix*, Fig. S4 *A* and *B*). Furthermore, high-frequency stimulation rendered low actin velocity, whereas low-frequency stimulation allowed for higher speed during the off times (*SI Appendix*, Fig. S4*C*). We further compared these effects with the dynamics of actin cytoskeleton on wtNSCs exposed to substrates of different stiffnesses. Interestingly, we found that actin velocity is significantly higher in cells seeded on soft substrates compared to stiff substrates (*SI Appendix*, Fig. S4 *D* and *E*). Our data indicate that, as with cell fate instruction, high-frequency activation of RhoA or Cdc42 mimics the effects of stiff matrices on actin cytoskeleton dynamics in NSCs, whereas low-frequency activation phenocopies NSCs exposed to soft substrates. We hypothesize that, when exposed to soft substrates, most of the Rho GTPases in these cells will exhibit scarce pulses of activation, leading to the formation of less stable, presumably shorter, actin filaments, rendering a more fluid cytoskeletal network (*SI Appendix*, Fig. S4*F*). Upon higher extracellular stiffness, the increase in Rho GTPase activation frequency would trigger stable actin filament formation, rendering a more static cytoskeletal organization (*SI Appendix*, Fig. S4*F*).

Frequency-Dependent Oscillatory Activation of Rho GTPases Controls SMAD1/5 Phosphorylation and Nuclear Translocation Dynamics in NSCs. We next examined how pulsatile activation of RhoA/Cdc42 and concomitant modulation of actin cytoskeleton dynamics are further transduced downstream into signals that irreversibly determine stem cell commitment. We first investigated effects on β-catenin signaling, as we have mechanistically linked the inhibition of this pathway in NSCs to stiffness-dependent reduction in neurogenesis (15). We used a β-catenin reporter composed of luciferase placed under the control of a β-catenin-responsive promoter (6xTCF) into NSCs (15); however, we did not detect any significant differences in luciferase activity upon Rho or Cdc42 activation during the critical temporal window, suggesting that a different mechanism may be involved (*SI Appendix*, Fig. S5*A*).

Rho GTPases have been shown to crosstalk with the transforming growth factor beta (TGF-β)/bone morphogenetic protein (BMP) signaling network, which controls the activation of the SMAD family of transcription factors (32–35). We and others have shown that these pathways are key regulators of NSC differentiation during both embryogenesis and adulthood (34, 36, 37). In addition, RhoA has been shown to mediate TGFβ-induced smooth muscle differentiation by modulating SMAD activity (32). We therefore investigated whether the SMAD pathway was playing a role in RhoA/Cdc42-mediated cell fate instruction. We seeded wtNSCs on compliant or rigid substrates and measured SMAD1/5 phosphorylation during the critical mechanosensitive time window. Remarkably, the proportion of cells positive for nuclear pSMAD1/5 was significantly higher on cells exposed to stiff substrates compared to those on soft matrices (*SI Appendix*, Fig. S5 *B* and *C*), indicating that matrices with higher elastic modulus promote activation of the SMAD1/5 pathway.

We next asked whether dynamic Rho GTPase activation within the mechanosensitive temporal window modulates SMAD1/5 activity. optoRhoA, optoCdc42, or wtNSCs were seeded on soft substrates and illuminated either constantly or at different frequencies for a total of 90 min, during the critical temporal window. Interestingly, we found that constant light stimulation of RhoA and Cdc42 triggered phosphorylation and nuclear translocation of SMAD1/5 (Fig. 5 *A*–*C*). In addition, low-frequency oscillation likewise induced SMAD1/5 phosphorylation and nuclear translocation (Fig. 5 *A*–*C*), where 45 min in the dark followed by a 45-min illumination induced significant SMAD1/5 phosphorylation and nuclear translocation compared to the dark control (Fig. 5 *A*–*C*). However, the inverse sequence (a 45-min light pulse followed by a 45-min dark pulse) did not yield noticeable SMAD1/5 phosphorylation or nuclear translocation, indicating that a 45-min gap in Rho GTPase activation is sufficient for SMAD1/5 activity to decay to background levels. In contrast, a 90-min total illumination at a high, 15-min on/off frequency, led to high levels of SMAD1/5 activity, regardless of illumination phase (Fig. 5 *A*–*C*). These results indicate that high-frequency Rho GTPase activation leads to persistent, whereas low-frequency activation leads to intermittent SMAD1/5 phosphorylation and nuclear localization.

It was recently shown in human embryonic stem cells that increased cellular contractility triggers SMAD1/5 phosphorylation, an effect that persisted in the presence of canonical inhibitors of TGF-β and BMP receptors (SB-431542 and LDN-193189), suggesting that noncanonical, receptor-independent mechanisms may be involved in this mechanotransduction (38). We thus likewise explored whether the effects of RhoA or Cdc42 activation on SMAD1/5 phosphorylation in NSCs were mediated by TGF-β/BMP receptors. We treated the optostimulated cells with the TGF-β receptor ALK4/5/7 inhibitor (SB-431542) and BMP-receptor ALK2/3 inhibitor (LDN-193189) and found that these did not block SMAD1/5 phosphorylation (*SI Appendix*, Fig. S5 *D* and *E*), suggesting that Rho GTPase activation may trigger SMAD1/5 phosphorylation via a mechanism independent of TGF-β/BMP receptors.

We next investigated whether Rho GTPase–triggered actin cytoskeleton reorganization was necessary for SMAD1/5 phosphorylation. Blocking actin cytoskeleton polymerization with CytoD inhibited the phosphorylation of nuclear SMAD1/5 in response to RhoA or Cdc42 activity (Fig. 6 *A* and *B*), indicating that an intact actin cytoskeleton is necessary for SMAD1/5 phosphorylation downstream of dynamic Rho GTPase activation.

Actin-Dependent SMAD1 Activity Mediates Stem Cell Fate Decisions Driven by Pulsatile Rho-GTPase Activation and Substrate Stiffness. We next examined whether SMAD1/5 is necessary to mediate the effect of dynamic Rho GTPase activation on fate commitment. Western blot and immunocytochemistry analyses readily detected SMAD1 expression in NSCs, whereas SMAD5 could not be detected to the same extent, at least with the antibody used for these assays, suggesting a higher expression of SMAD1 over SMAD5 in these cells (*SI Appendix*, Fig. S6 *A* and *B*). We thus disrupted SMAD1 expression via an shRNA-mediated knockdown (KD) in optoRhoA NSCs. The most effective shRNA tested ("shRNA SMAD1.2") resulted in a nearly 80% reduction in SMAD1 protein levels (*SI Appendix*, Fig. S6*C*), and we generated stable optoRhoA NSCs SMAD1 KD cells ("shSMAD1.2-optoRhoA" NSCs). We next subjected these cells, alongside an RNAi control cell line ("shLacZ-optoRhoA" NSCs), to either high- or low-frequency RhoA activation during

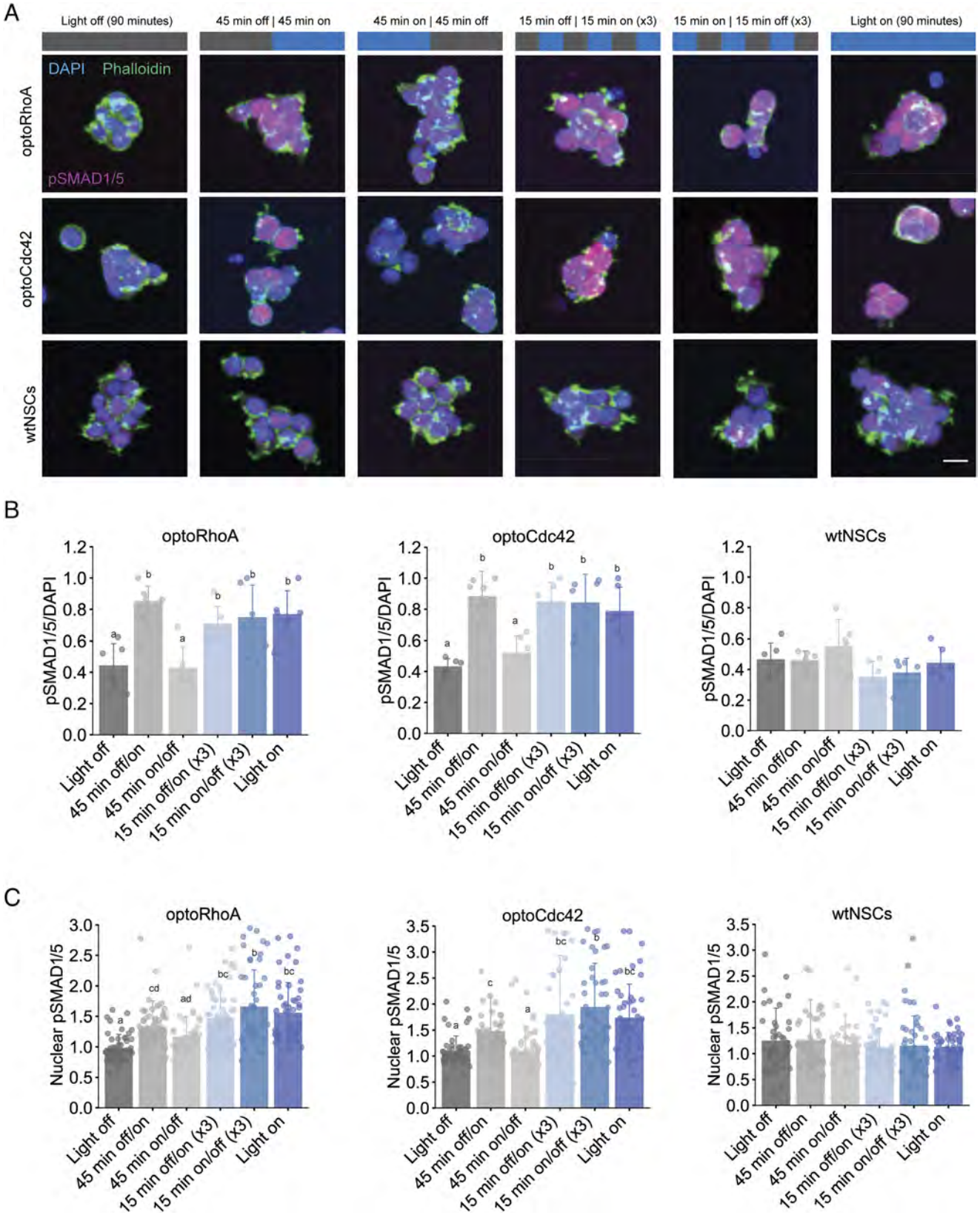

Fig. 5. SMAD1/5 phosphorylation and nuclear localization is modulated by the frequency of activation of Rho GTPases. (*A*) Immunostaining for pSMAD1/5 Ser463/465, phalloidin, and DAPI in NSCs seeded on soft hydrogels and illuminated at the indicated frequencies for 90 min. Average light dose for all conditions was 0.5 μW/mm^2. (Scale bar, 10 μm.) (*B*) Quantification of *A*. pSMAD1/5+/DAPI ratios were calculated. Data are mean ± SD (n = 6 biological replicates). One-way ANOVA with Tukey's multiple comparison test was used to evaluate significance. (*C*) Quantification of *A*. Using Fiji, masks of cell nuclei were generated to segment nuclear from cytoplasmic signal. Mean pSMAD1/5 nuclear/cytoplasmic intensity ratios are plotted. Data are mean ± SD (n = 50 cells per condition). One-way ANOVA with Tukey's multiple comparison test was used to evaluate significance.

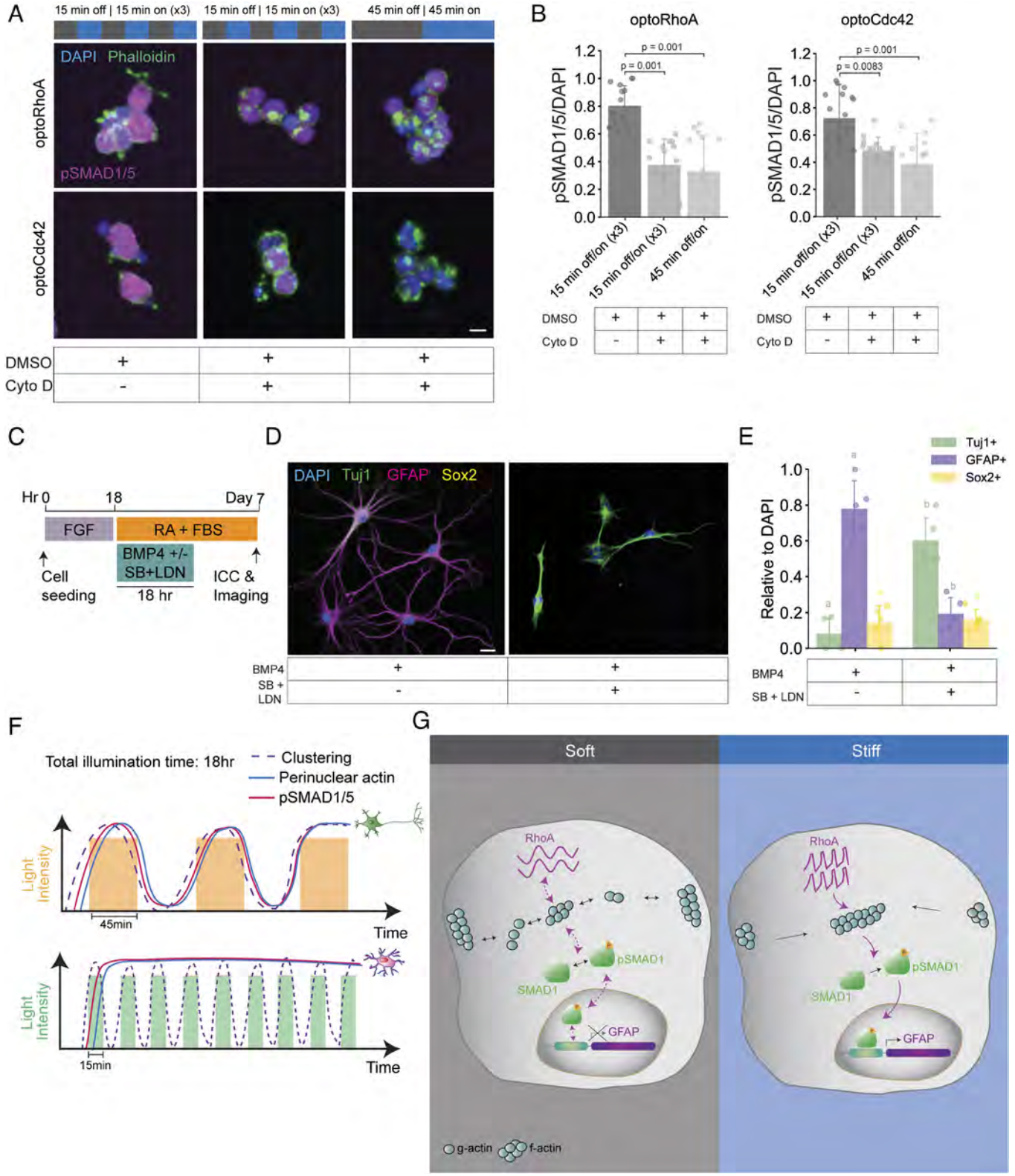

Fig. 6. Actin-dependent activation of SMAD1 signaling pathway mediates the effects of dynamic activation of RhoA and Cdc42 on cell fate. (*A*) Immunostaining for pSMAD1/5 Ser463/465, phalloidin, and DAPI in NSCs seeded on soft hydrogels and illuminated at the indicated frequencies for a total of 90 min in the presence of CytoD or vehicle control (DMSO). Average light dose for all conditions was 0.5 μW/mm^2. (Scale bar, 10 μm.) (*B*) Quantification of *A*. pSMAD1/5+/DAPI ratios were calculated. Data are mean ± SD (n = 10 to 15 biological replicates). One-way ANOVA with Tukey's multiple comparison test was used to evaluate significance. (*C*) Media conditions and optostimulation pattern used. SMAD pathway was activated with rhBMP-4 (100 ng/mL, R&D Systems) and/or inhibited with LDN-193189 ("LDN," 100 nM, R&D Systems) or SB-431542 ("SB," 10 μm, R&D Systems). (*D*) Immunostaining in NSCs treated as indicated for 18 h and fixed after 7 d of differentiation. (Scale bar, 10 μm.) (*E*) Quantification of *E*. Tuj1+/DAPI, GFAP+/DAPI, and Sox2/DAPI ratios were calculated. Data are mean ± SD (n = 5 biological replicates). Student's *t* test was used to evaluate significance. (*F*) Frequency-dependent activation of Rho GTPases renders differential effects on cytoskeletal dynamics and SMAD1/5 activation in NSCs. (*G*) Proposed model for mechanosensitive dynamic activation of Rho GTPases. High-frequency activation renders astrocytic fates through persistent activation of the SMAD1/5 pathway.

the critical 18-h window, then determined their cell fate after 7 d (*SI Appendix*, Fig. S6*D*). As anticipated, control cells (shLacZ-optoRhoA) exposed to high-frequency activation of RhoA showed a marked inhibition of neurogenesis and promotion of astrogenesis compared to cells subjected to low-frequency stimulation of RhoA (*SI Appendix*, Fig. S6 *E* and *F*). However, SMAD1 KD eliminated the differences in the proportions of neurons and astrocytes generated between high-frequency activation conditions and low-frequency conditions (*SI Appendix*, Fig. S6 *E* and *F*), indicating that this transcription factor mediates the frequency-dependent RhoA impact on cell fate decisions.

To further elucidate the role of the SMAD1 pathway on fate commitment in wtNSCs, we used BMP4, a canonical activator of this pathway that binds to type I receptors ALK1/2 and ALK3 and type II receptor BMPR2, triggering downstream phosphorylation of SMAD1/5 (39, 40). Recombinant BMP4 treatment of wtNSCs just during the critical 18-hour window strongly shifted cell fate toward astrocytes (Fig. 6 *C*–*E*). We further found that addition of TGF-β/BMP receptor inhibitors (LDN-193189 and SB431542) reversed these effects of BMP4 treatment (Fig. 6 *C*–*E*).

Altogether, these results suggest that stiff matrices increase RhoA and Cdc42 activation frequency, which in turn enhances actin assembly needed to trigger persistent SMAD1/5 activation, rendering a shift in cell commitment toward astrocytic fates. In contrast, softer matrices reduce the frequency of RhoA and Cdc42 activation, producing a more dynamic actin and transiently assembled actin cytoskeleton and reducing SMAD1/5 phosphorylation, and neurogenesis. Critically, we found that the effect of matrix stiffness can be phenocopied by optogenetic stimulation of RhoA and Cdc42 at the appropriate frequency (Fig. 6 *F* and *G*).

Discussion

Cells actively sense biophysical cues from the extracellular space through dynamic generation of protrusions coordinated by Rho GTPases. These mechanotransduction proteins are molecular switches that cycle between active and inactive forms in response to mechanical inputs in all mechanosensitive cell types, modulating proliferation, protrusion extension, and cell migration (41). Moreover, work from our and other groups has shown that steady activation of Rho GTPases mediates stiffness-instructed cell fate decisions in NSCs and MSCs, indicating that these proteins are also critical mediators of mechanosensitive differentiation (14, 21). While these studies clearly demonstrate that substrate stiffness influences the *magnitude* of Rho GTPase activation, it is unclear whether the *dynamics* are also affected. Here, we used FRET-based Rho biosensors and biochemical assays to reveal that Rho GTPases exhibit oscillatory activation dynamics in NSCs, and that the frequency of these oscillations is modulated by the elastic properties of the underlying matrix (Fig. 6 *F* and *G*). In addition, the frequency of oscillatory RhoA or Cdc42 activation during a critical temporal window of mechanosensitivity dictates stem cell fate through a mechanism that involves modulation of actin cytoskeleton dynamics and downstream dynamic activation of SMAD1/5, which promotes an astrocytic over neuronal fate.

Using RhoA biosensors, we revealed that active RhoA fluctuates at a low frequency in NSCs seeded on soft substrates, with peaks repeating every ~45 to 60-min, and this frequency is approximately four times higher when cells are seeded on stiff matrices (~5 to 10-min periods). Osteosarcoma cells have been recently found to exhibit spontaneous pulsatile activation of Rho GTPases, with a period in the order of ~5-min, which agrees in order of magnitude with our data shown here for NSCs seeded on stiff substrates (4, 11). Generation of spontaneous protrusions coupled to oscillatory activation of Ras GTPases was recently shown for breast cancer cells, acting as a pacemaker for triggering downstream pulses of ERK activation (9).

While a number of stem cells are known to undergo mechanosensitive lineage commitment via mechanisms involving Rho GTPases (21, 42), we demonstrate that Rho undergoes stiffness-dependent dynamic fluctuations and that these fluctuations are important for cell fate determination. Given that Ras and Rho GTPase oscillations have been recently described for other cell types, it is tempting to speculate that frequency-modulated oscillations in Rho GTPase activity in response to substrate stiffness described here for NSCs could represent a widespread mechanism shared among other mechanosensitive proteins in diverse cellular contexts. As has been suggested before (11), a functional advantage of oscillatory activation dynamics of these GTPases is that they offer a mechanism for cells to continuously probe their environment via dynamic cell contractions and mechanosensitive focal adhesions, and therefore more efficiently adapt to dynamically changing extracellular mechanical forces, in this case during the mechanosensitive time window. In addition, localized RhoA activation and downstream contraction pulses, as opposed to whole-cell activation of Rho GTPases, enable local sensing of dynamic extracellular cues while preventing global contraction of the entire cell, which could otherwise lead to detachment from its matrix.

We revealed that tuning the frequency of pulsatile optogenetic activation of RhoA and Cdc42 within the first few hours of differentiation induces the same differentiation profile obtained by varying substrate stiffness, with low-frequencies resembling soft substrates and high-frequencies phenocopying the effects of stiff matrices. Notably, the spatial distribution of active RhoA/Cdc42 throughout the cytoplasm and plasma membrane regions revealed by FRET resembles clusters of activation achieved by optogenetic stimulation of these proteins. Further studies using biosensors to determine subcellular localization of active endogenous Rho GTPase would be informative to confirm the subcellular distribution of these protein domains. Analogously, the future use of optogenetic systems that enable spatial control of Rho GTPase activation with subcellular resolution would reveal whether individual domains of Rho GTPases may control distinct cellular functions. The variable frequency of Rho GTPase fluctuations we observed modulated actin cytoskeleton dynamics and determined downstream SMAD1/5 phosphorylation and nuclear translocation patterns. SMADs are a family of transcription factors that lie at the core of the TGFβ and BMP pathways, with critical roles in embryogenesis for neuroectoderm patterning during cerebral cortex development (43). In the adult brain, activation of the SMAD pathway inhibits neurogenesis (36, 37) and has been recently linked to astrocytic promotion, though the underlying mechanism remains to be elucidated (35). Our results support a role of SMAD1/5 downstream of RhoA and Cdc42 activation during a critical window of mechanosensitivity in instructing astrogenesis over neurogenesis in NSCs.

Modulation of temporal dynamics in SMAD1/5 phosphorylation and nuclear translocation in response to the frequency of pulsatile optogenetic activation of Rho GTPases suggests that a persistent nuclear localization of pSMAD1/5 is required to shift cell commitment from neuronal to astrocytic fates, whereas sparse pulses of SMAD1/5 activation were not sufficient for astrogenesis. Seminal work investigating the temporal regulation of

transcription factors demonstrated that activation of factors such as NF-kappaB in lymphocytes is sensitive to the frequency of intracellular calcium concentration oscillations, driving phenotypic outcomes ranging from interleukin secretion to differentiation (44).

Overall, our data strongly support a role for the Rho GTPase activation dynamics in processing stiffness cues and instructing mechanosensitive stem cell differentiation. These effects can be phenocopied by optogenetic stimulation of RhoA and Cdc42 at the appropriate frequency. These findings advance our fundamental understanding of how ECM mechanics influence cell fate and could further aid in the development of unique strategies to control the timing of biophysical differentiation cues and modulation of Rho and SMAD signaling pathways for improved stem cell lineage manipulation, which remains an essential challenge for regenerative therapies.

Materials and Methods

Detailed experimental methods including culture of NSCs, PA gel preparation, optogenetic stimulation, live-cell imaging, and single-cell microisland array technology can be found in *SI Appendix*.

Data, Materials, and Software Availability. All study data, protocols and scripts are included in the article and/or *SI Appendix*.

ACKNOWLEDGMENTS. We thank Dr. Mary West and Holly Aaron for their technical support. This work was supported by the NIH (R01NS074831 to S.K. and D.V.S.) and Siebel Postdoctoral Fellowship to R.G.S. Imaging at the Cancer Research Laboratory (CRL) Molecular Imaging Center, RRID:SCR_017852, was supported by Helen Wills Neuroscience Institute.

Author affiliations: [a]Department of Chemical and Biomolecular Engineering, University of California, Berkeley, CA 94720; and [b]Department of Bioengineering, University of California, Berkeley, CA 94720

1. F. H. Gage, Mammalian neural stem cells. *Science* **287**, 1433–1438 (2000).
2. G. Kempermann *et al.*, Human adult neurogenesis: Evidence and remaining questions. *Cell Stem Cell* **23**, 25–30 (2018).
3. K. Saha *et al.*, Substrate modulus directs neural stem cell behavior. *Biophys. J.* **95**, 4426–4438 (2008).
4. D. Kamps *et al.*, Optogenetic tuning reveals rho amplification-dependent dynamics of a cell contraction signal network. *Cell Rep.* **33**, 108467 (2020).
5. K. I. Mosher, D. V. Schaffer, Influence of hippocampal niche signals on neural stem cell functions during aging. *Cell Tissue Res.* **371** (2018).
6. M. Javier-Torrent, G. Zimmer-Bensch, L. Nguyen, Mechanical forces orchestrate brain development. *Trends Neurosci.* **44**, 110–121 (2021).
7. P. Nalbant, L. Dehmelt, Exploratory cell dynamics: A sense of touch for cells? *Biol. Chem.* **399**, 809–819 (2018).
8. B. L. Doss *et al.*, Cell response to substrate rigidity is regulated by active and passive cytoskeletal stress. *Proc. Natl. Acad. Sci. U.S.A.* **117**, 12817–12825 (2020).
9. J. M. Yang *et al.*, Integrating chemical and mechanical signals through dynamic coupling between cellular protrusions and pulsed ERK activation. *Nat. Commun.* **9**, 1–13 (2018).
10. M. C. Weiger *et al.*, Spontaneous phosphoinositide 3-kinase signaling dynamics drive spreading and random migration of fibroblasts. *J. Cell Sci.* **122**, 313–323 (2009).
11. M. Graessl *et al.*, An excitable Rho GTPase signaling network generates dynamic subcellular contraction patterns. *J. Cell Biol.* **216**, 4271–4285 (2017).
12. S. Phuyal, H. Farhan, Multifaceted Rho GTPase signaling at the endomembranes. *Front. Cell Dev. Biol.* **7**, 127 (2019).
13. C. H. Huang, M. Tang, C. Shi, P. A. Iglesias, P. N. Devreotes, An excitable signal integrator couples to an idling cytoskeletal oscillator to drive cell migration. *Nat. Cell Biol.* **15**, 1307–1316 (2013).
14. A. J. Keung, E. M. De Juan-Pardo, D. V. Schaffer, S. Kumar, Rho GTPases mediate the mechanosensitive lineage commitment of neural stem cells. *Stem Cells* **29**, 1886–1897 (2011).
15. S. Rammensee, M. S. Kang, K. Georgiou, S. Kumar, D. V. Schaffer, Dynamics of mechanosensitive neural stem cell differentiation. *Stem Cells* **35**, 497–506 (2017).
16. G. Berdugo-Vega *et al.*, Increasing neurogenesis refines hippocampal activity rejuvenating navigational learning strategies and contextual memory throughout life. *Nat. Commun.* **11**, 1–12 (2020).
17. J. T. Gonçalves, S. T. Schafer, F. H. Gage, Adult neurogenesis in the hippocampus: From stem cells to behavior. *Cell* **167**, 897–914 (2016).
18. N. Antonovaite, S. V. Beekmans, E. M. Hol, W. J. Wadman, D. Iannuzzi, Regional variations in stiffness in live mouse brain tissue determined by depth-controlled indentation mapping. *Sci. Rep.* **8**, 12517 (2018).
19. T. Luque, M. S. Kang, D. V. Schaffer, S. Kumar, Microelastic mapping of the rat dentate gyrus. *R. Soc. Open Sci.* **3**, 150702 (2016).
20. C. Yang, M. W. Tibbitt, L. Basta, K. S. Anseth, Mechanical memory and dosing influence stem cell fate. *Nat. Mater.* **13**, 645–652 (2014).
21. R. McBeath, D. M. Pirone, C. M. Nelson, K. Bhadriraju, C. S. Chen, Cell shape, cytoskeletal tension, and RhoA regulate stem cell lineage commitment. *Dev. Cell* **6**, 483–495 (2004).
22. L. J. Bugaj, A. T. Choksi, C. K. Mesuda, R. S. Kane, D. V. Schaffer, Optogenetic protein clustering and signaling activation in mammalian cells. *Nat. Methods* **10**, 249–252 (2013).
23. R. D. Fritz *et al.*, A versatile toolkit to produce sensitive FRET biosensors to visualize signaling in time and space. *Sci. Signal.* **6**, rs12 (2013).
24. P. Ekblom, P. Lonai, J. F. Talts, Expression and biological role of laminin-1. *Matrix Biol.* **22**, 35–47 (2003).
25. L. J. Bugaj, A. T. Choksi, C. K. Mesuda, R. S. Kane, D. V. Schaffer, Optogenetic protein clustering and signaling activation in mammalian cells. *Nat. Methods* **10**, 249–252 (2013).
26. N. A. Repina *et al.*, Engineered illumination devices for optogenetic control of cellular signaling dynamics. *Cell Rep.* **31**, 107737 (2020).
27. N. A. Repina, H. J. Johnson, T. McClave, R. S. Kane, D. V. Schaffer, Protocol to fabricate engineered illumination devices for optogenetic control of cellular signaling dynamics. *STAR Protoc.* **1**, 100141 (2020).
28. W. Zhang, Y. Huang, S. J. Gunst, The small GTPase RhoA regulates the contraction of smooth muscle tissues by catalyzing the assembly of cytoskeletal signaling complexes at membrane adhesion sites. *J. Biol. Chem.* **287**, 33996–34008 (2012).
29. S. J. Heasman, A. J. Ridley, Mammalian Rho GTPases: New insights into their functions from in vivo studies. *Nat. Rev. Mol. Cell Biol.* **9**, 690–701 (2008).
30. S. Chen *et al.*, Interrogating cellular fate decisions with high-throughput arrays of multiplexed cellular communities. *Nat. Commun.* **7**, 10309 (2016).
31. J. M. Encinas *et al.*, Division-coupled astrocytic differentiation and age-related depletion of neural stem cells in the adult hippocampus. *Cell Stem Cell* **8**, 566–579 (2011).
32. S. Chen *et al.*, RhoA modulates Smad signaling during transforming growth factor-β-induced smooth muscle differentiation. *J. Biol. Chem.* **281**, 1765–1770 (2006).
33. D. Kardassis, C. Murphy, T. Fotsis, A. Moustakas, C. Stournaras, Control of transforming growth factor signal transduction by small GTPases. *FEBS J.* **276**, 2947–2965 (2009).
34. J. Stipursky *et al.*, TGF-Î²1 promotes cerebral cortex radial glia-astrocyte differentiation in vivo. *Front. Cell. Neurosci.* **8**, 393 (2014).
35. S. Qin, W. Niu, N. Iqbal, D. K. Smith, C. L. Zhang, Orphan nuclear receptor TLX regulates astrogenesis by modulating BMP signaling. *Front. Neurosci.* **8**, 74 (2014).
36. H. Yousef *et al.*, Systemic attenuation of the TGF-β pathway by a single drug simultaneously rejuvenates hippocampal neurogenesis and myogenesis in the same old mammal. *Oncotarget* **6**, 11959–11978 (2015).
37. H. Yousef *et al.*, Age-associated increase in BMP signaling inhibits hippocampal neurogenesis. *Stem Cells.* **33**, 1577–1588 (2015).
38. X. Xue *et al.*, Mechanics-guided embryonic patterning of neuroectoderm tissue from human pluripotent stem cells. *Nat. Mater.* **17**, 633–641 (2018), 10.1038/s41563-018-0082-9 (27 June 2021).
39. X. Qi *et al.*, BMP4 supports self-renewal of embryonic stem cells by inhibiting mitogen-activated protein kinase pathways. *Proc. Natl. Acad. Sci. U.S.A.* **101**, 6027–6032 (2004).
40. F. Dituri, C. Cossu, S. Mancarella, G. Giannelli, The interactivity between TGFβ and BMP signaling in organogenesis, fibrosis, and cancer. *Cells* **8**, 1130 (2019).
41. A. Hall, G. Lalli, Rho and Ras GTPases in axon growth, guidance, and branching. *Cold Spring Harb. Perspect. Biol.* **2**, a001818 (2010).
42. H. Lv *et al.*, Mechanism of regulation of stem cell differentiation by matrix stiffness. *Stem Cell Res. Ther.* **6**, 103 (2015).
43. L. Menendez, T. A. Yatskievych, P. B. Antin, S. Dalton, Wnt signaling and a Smad pathway blockade direct the differentiation of human pluripotent stem cells to multipotent neural crest cells. *Proc. Natl. Acad. Sci. U.S.A.* **108**, 19240–19245 (2011).
44. R. E. Dolmetsch, K. Xu, R. S. Lewis, Calcium oscillations increase the efficiency and specificity of gene expression. *Nature* **392**, 933–936 (1998).